

CONF-9510276--1

RECEIVED

JAN 08 1996

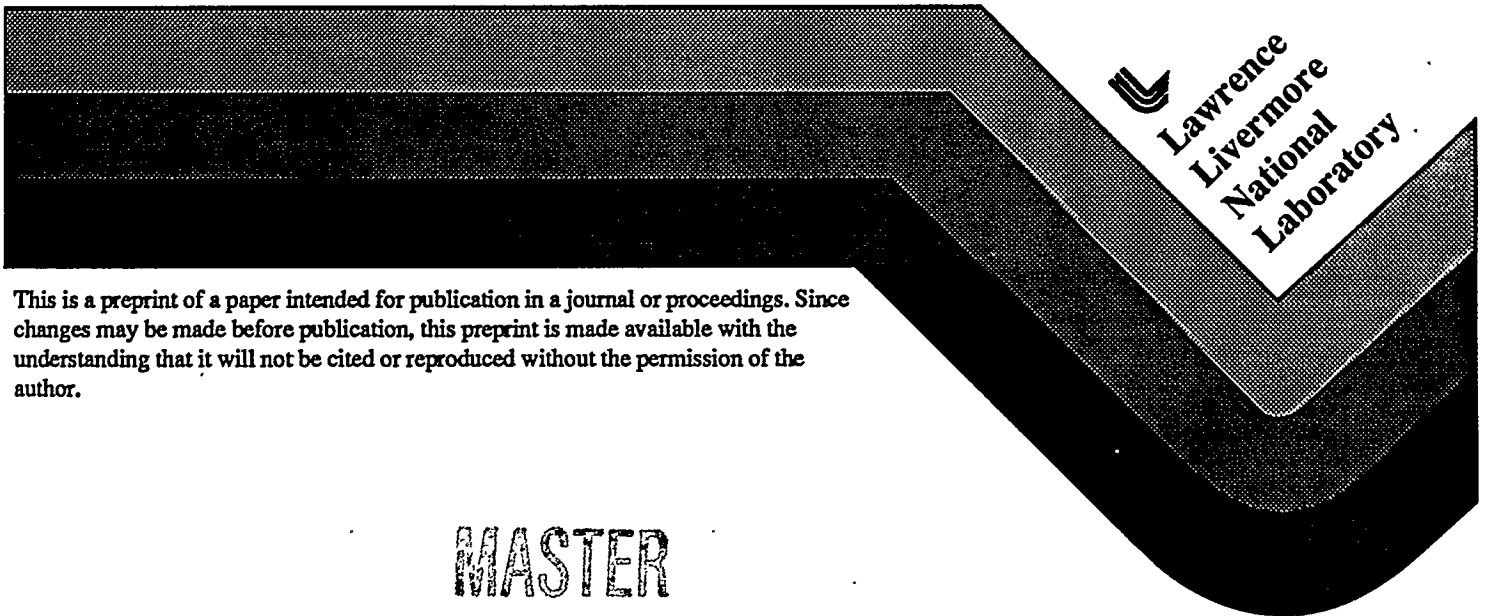
OSTI

Inference of the Potential Predictability of Seasonal Land-Surface Climate from AMIP Ensemble Integrations

Thomas J. Phillips and Benjamin D. Santer
Program for Climate Model Diagnosis and Intercomparison (PCMDI)
Lawrence Livermore National Laboratory
Livermore, CA 94551

This paper was prepared for the
Proceedings of the 20th Annual Climate Diagnostics Workshop
Seattle, Washington
23-27 October 1995

December 1995



This is a preprint of a paper intended for publication in a journal or proceedings. Since changes may be made before publication, this preprint is made available with the understanding that it will not be cited or reproduced without the permission of the author.

MASTER

DISTRIBUTION OF THIS DOCUMENT IS UNLIMITED

SECRET
CONFIDENTIAL

DISCLAIMER

This document was prepared as an account of work sponsored by an agency of the United States Government. Neither the United States Government nor the University of California nor any of their employees, makes any warranty, express or implied, or assumes any legal liability or responsibility for the accuracy, completeness, or usefulness of any information, apparatus, product, or process disclosed, or represents that its use would not infringe privately owned rights. Reference herein to any specific commercial products, process, or service by trade name, trademark, manufacturer, or otherwise, does not necessarily constitute or imply its endorsement, recommendation, or favoring by the United States Government or the University of California. The views and opinions of authors expressed herein do not necessarily state or reflect those of the United States Government or the University of California, and shall not be used for advertising or product endorsement purposes.

Inference of the Potential Predictability of Seasonal Land-Surface Climate from AMIP Ensemble Integrations

Thomas J. Phillips (phillips@twworks.llnl.gov) and Benjamin D. Santer
Program for Climate Model Diagnosis and Intercomparison (PCMDI)
Lawrence Livermore National Laboratory
Livermore, California

1. Introduction

A number of recent studies of the potential predictability of seasonal climate have utilized AGCM ensemble integrations--i.e., experiments where the atmospheric model is driven by the same ocean boundary conditions and radiative forcings, but is started from different initial states. However, only a few variables of direct relevance to the climate of the land surface (the key locus of human interaction with climate) have been examined. In this study, we infer the potential predictability of 11 climate variables that are indicative of the energetics, dynamics, and hydrology of the land surface (see first column of the Table).

We used a T42L19 ECMWF (cycle 36) AGCM having a land-surface scheme with prognostic temperature and moisture of 2 layers occupying the topmost 0.50 meters of soil, but with monthly climatological values of these fields prescribed below. Six model realizations of decadal climate (for the period 1979-1988) were considered. In each experiment, the SSTs and sea ice extents were those specified for the Atmospheric Model Intercomparison Project (AMIP), and some radiative parameters were prescribed as well (i.e., solar constant = 1365 W m^{-2} ; global CO_2 concentration = 345 ppm). However, the initial conditions of the model atmosphere and land surface were different: the first two simulations were initialized from ECMWF analyses, while the initial states of subsequent realizations were assigned values that were the same as those at the last time step of the preceding integration.

2. Methodology

The potential predictability of seasonal climate is often expressed as a ratio of temporal variances:

$$\{ \sigma_T^2 - \sigma_I^2 \} / \sigma_I^2$$

Here σ_I^2 is that part of the total temporal variance σ_T^2 that is attributable to the (unpredictable) internal variability of the climate, which can be estimated from an ensemble of model realizations which vary only in initial conditions. Instead, we inferred the potential predictability of land-surface variables by different measures that more fully utilized the spatio-temporal information available from 6 model realizations. Moreover, because our statistical measures were based on correlations between independent pairs of these realizations, the ensemble size was effectively expanded from $n = 6$ to $N = 15$ (i.e., $n!/[2!(n-2)!]$) members.

Because the potential predictability of seasonal climate implies the ability to forecast *inter-annual variability*, we analyzed the individual seasonal anomaly departures $A(x,y,t)$ of each land-surface variable from the 10-year climatological seasonal cycle--i.e., a time series of ~ 40 anomaly departure maps $A(x,y)$. Our statistical measures included:

- Zero-lag temporal correlations $r(x,y)$ computed at each land grid point (x,y) between pairs of anomaly time series $A(x,y,t)$ of like land-surface variables
- Pattern correlations $s(t)$ computed on land points at each time point t for the same anomaly pairs
- Global measure R , an area-weighted spatial average of $r(x,y)$ over all (~2700) land points (x,y)

- Global measure S , a time average of $s(t)$ over all (~ 40) time points t
- Root-mean-square (RMS) global measure $RS = [(R^2 + S^2)/2]^{1/2}$

For each of these measures, an ensemble mean μ and intraensemble spread δ were computed from $N = 15$ samples.

Because all these statistics are measures of temporal or spatial *similarity* among the seasonal anomalies of the different realizations of climate, they are *inversely* related to the unpredictable internal variability of the model. It can thus be assumed that the larger the value of the ensemble mean μ of a correlation statistic, and the smaller its intraensemble spread δ , the greater is the associated potential predictability of the seasonal anomalies of the variable. (The inherent weakness of these statistics is that they are measures only of the similarity in temporal or spatial *phase* among the realizations. However, we also examined *amplitude-sensitive* measures of potential predictability such as the variance ratio in the first equation of this section. These results, which present a somewhat brighter picture of the potential predictability of a few land-surface variables in certain seasons, will be reported in a future paper.)

3. Results

Maps of μ and δ of temporal correlations $r(x,y)$ reveal that seasonal continental climate is much more predictable in the tropics--notably over Amazonia, Equatorial Africa, Southern Asia, and Northern Australia (e.g., see maps of Figure 1 for mean sea-level pressure--MSLP). Over extratropical continents, the correlations are mostly < 0.5 for all 11 variables, and some (e.g., surface evaporation, sensible heat flux, and wind stresses) show substantial areas of temporal *anticorrelation* (not shown). These results imply that in the extratropics no one model realization can accurately predict the anomalies of a particular season; however, averaging over an ensemble of realizations can substantially increase the probability of obtaining accurate extratropical seasonal forecasts (Palmer and Anderson 1994, Barnett 1995).

Even in the tropics, there is a considerable range of potential predictability among the model's land-surface variables. For example, tropical MSLP shows broad areas of temporal correlations > 0.5 (Figure 1), while correlations of surface evaporation are this high in only a few scattered equatorial regions (not shown). (Correlations > 0.5 indicate a *practically significant* predictability that would be of potential social value. It should be noted, however, that an ensemble-mean correlation of 0.5 implies that only 25 % of the interannual variance of a seasonal land-surface variable in a given realization is explained, on average, by another realization.)

The time series of μ and δ for the pattern correlation $s(t)$ of the 11 land-surface variables reveals quite different phenomena. In this case, MSLP exhibits numerous instances of negative-valued ensemble-mean $s(t)$ and generally large intraensemble spread δ (not shown), while the surface evaporation shows substantially more coherence (Figure 2). There is also an obvious enhancement of the ensemble-mean pattern correlations of surface evaporation in seasons immediately following the onset of El Niño and La Niña events (e.g. 1982/83, 1984/85, 1986/87). The ENSO signal is present in the pattern correlations of seasonal anomalies of all the other land-surface variables, suggesting that continental seasonal climate is generally more predictable at such times.

The potential predictability of different land-surface variables ranges rather widely in a global sense as well (see Table). The model's soil moisture, MSLP, and surface air temperature are most predictable overall, while the surface fluxes of momentum, sensible heat, and moisture are the least predictable. The hydrological variables and those related to the radiation and temperature at the ground show intermediate levels of global potential predictability.

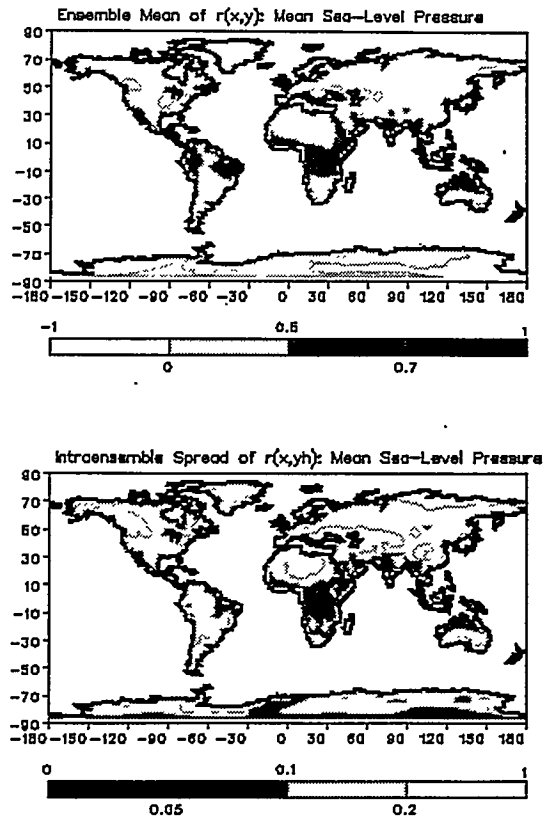


Figure 1: Maps of ensemble mean μ (top) and intraensemble spread δ (bottom) of zero-lag temporal correlations $r(x,y)$ between 15 pairwise-selected realizations of seasonal anomalies of continental mean sea-level pressure (MSLP). Note that darker shading in both panels indicates regions where MSLP is likely to be most predictable in a temporal sense (i.e., areas with relatively high ensemble-mean correlations and low intraensemble spread).

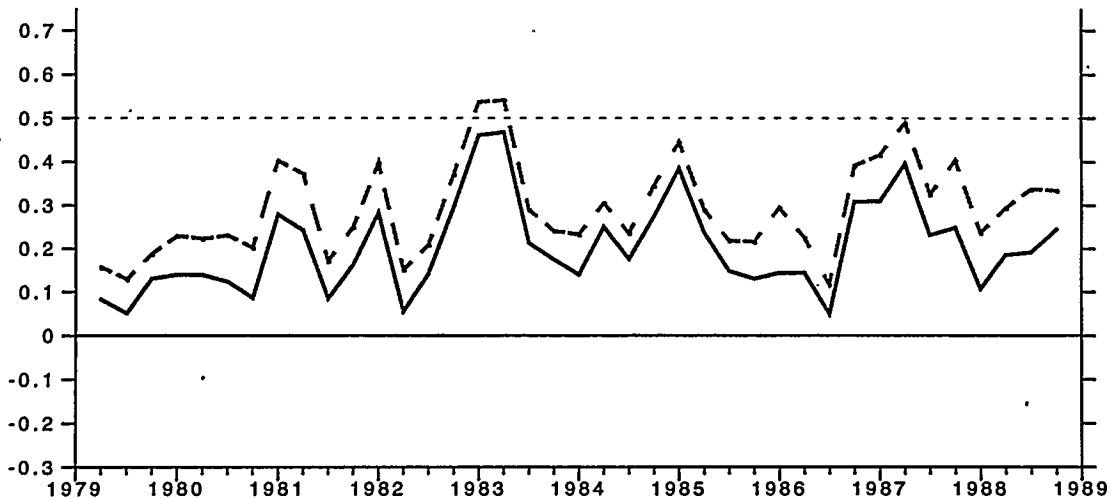


Figure 2: Time series of ensemble mean μ (solid line) and intraensemble spread δ (dashed line) of pattern correlations $s(t)$ between 15 pairwise-selected realizations of seasonal anomalies of continental surface evaporation.

Table: Global measures of the potential predictability of seasonal anomalies of 11 land-surface variables. The variables are ranked in order of the magnitude of the ensemble-mean rms global measure $RS = [(R^2 + S^2)/2]^{1/2}$, where R is an area-weighted average of temporal correlations $r(x,y)$ and S is a time average of pattern correlations $s(t)$.

Variable	RS	R	S
Soil Moisture	0.220	0.203	0.236
Mean Sea-Level Pressure (MSLP)	0.216	0.292	0.090
Surface Air Temperature	0.216	0.266	0.150
Precipitation	0.198	0.145	0.239
Surface Net SW Radiation	0.195	0.205	0.184
Surface Net LW Radiation	0.192	0.203	0.182
Ground Temperature	0.189	0.241	0.116
Surface U-Wind Stress	0.177	0.211	0.133
Surface Evaporation	0.176	0.143	0.203
Surface Sensible Heat Flux	0.172	0.153	0.188
Surface V-Wind Stress	0.155	0.187	0.113

It is likely that the relatively slow spatio-temporal variation of the model's soil moisture contributes to its higher global potential predictability. The apparent absence of a strong connection between the potential predictability of the model's seasonal anomalies of soil moisture and surface evaporation is probably due to the role that the simulated vegetation canopy plays in regulating evaporation. Moisture intercepted by the canopy evaporates directly to the atmosphere, while evapotranspiration of soil moisture is inhibited during times of vegetation stress, such as dry climatic conditions.

From the Table, it can be seen that the S values of seasonal anomalies of soil moisture, precipitation, evaporation, and sensible heat flux are higher than those of MSLP and surface air temperature, while the R values of the latter variables are higher than those of the former. This behavior appears to be related to differences in the characteristic spatial scales of the seasonal anomalies of different variables. For example, in different model realizations it is not unusual for MSLP anomalies in a particular season to be of opposite signs on a continental scale, thereby yielding low values of $s(t)$, and a low S value overall. The seasonal land-surface evaporation anomalies are generally of much smaller scale, so oppositely signed anomalies impact the pattern correlations much less. On the other hand, the temporal variation of the surface evaporation anomalies is more rapid (noisy) than that of the MSLP anomalies, so the R value of the latter is higher.

Some land-surface variables (e.g. MSLP, surface air temperature, precipitation, ground temperature, surface u-wind stress, surface evaporation) exhibit a pronounced asymmetry in their R and S values. We caution that this property may be merely an artifact of different sample sizes. That is, R is obtained by averaging $r(x,y)$ over ~ 2700 land points (x,y) , while S represents an average of $s(t)$ over only ~ 40 time points.

Acknowledgments. This work was performed under the auspices of the Department of Energy Environmental Sciences Division by the Lawrence Livermore National Laboratory under Contract W-7405-ENG-48.

References

- Barnett, T.P., 1995: Monte Carlo climate forecasting. *J. Climate*, **8**, 1005-1022.
- Palmer, T.N., and D.L.T. Anderson, 1994: The prospects for seasonal forcing—A review paper. *Quart. J. Roy. Meteor. Soc.*, **120**, 755-792.

